

EXTENDED KALMAN FILTER DESIGN USING BEARING AND TIME-TO-GO MEASUREMENT FOR A HOMING MISSILE GUIDANCE

Sang-Wook Shim*, Bong-Gyun Park**, Byoung-Ju Jeon*,
Min-Jea Tahk*, and Hyuck Hoon Kwon**

*Division of Aerospace Engineering, KAIST, Daejeon, Korea
(E-mail: {swshim, bjeon, mjtahk}@fdcl.kaist.ac.kr)

**PGM R&D Lab., LIG Nex1, Seongnam-City, Korea
(E-mail: {bonggyun.park, hhkwon22}@lignex1.com)

Keywords: *Time-to-go estimation, Expansion rate, Extended Kalman filter, Passive seeker*

Abstract

In this paper, we construct a filter dynamics using bearing angle and time-to-go measurements obtained from sequential image frames of a passive seeker. Typically, estimation filter with bearing-only measurement is used for missile guidance. However, seeker images include much more information such as target size and its expansion rate. Time-to-go measurements can be calculated by target size in image and its expansion rate. Therefore, we construct a guidance filter with additional time-to-go information. Time-to-go measurements are calculated by several image process. The process are illustrated in detail. As shown in the numerical results, the state estimation errors are reduced by using time-to-go measurement. The performances of filters using bearing-only measurement and using bearing and time-to-go measurement are compared by Monte-Carlo simulation.

1 Introduction

Over the past few decades, many optimal guidance laws have been developed to satisfy some terminal constraints. These optimal guidance laws are formulated with time-to-go information [1]-[3]. If the time-to-go estimation is incorrect, the performance of these guidance laws will be severely degraded and terminal

constraints could not be also satisfied. Therefore, estimating relative distance, velocity and actual time-to-go information is very significant problem of missile's guidance filter. To guarantee performance of the guidance law, estimation results of time-to-go and relative motion should be accurate.

For missiles with passive seekers, the bearing-only measurement is typically used for estimating missile's state. However, seeker images include much more information such as target size and its expansion rate. If we can use this additional information, we can estimate missile's states more accurately. Furthermore, bearing-only measurement does not guarantee observability of the guidance filter. The observability is closely related to the bearing angle rate or LOS rate. If the angle rate is nearly zero, the system loses its observability. Typical terminal guidance usually has less LOS rate as a missile close to the target. Therefore, alternative measurement is required to tackle this critical problem to implement optimal guidance laws for missiles with passive seeker.

In this paper, filter dynamics with bearing angle and time-to-go measurement for missile with passive image sensor are simulated to intercept ground stationary target. The bearing measurement and time-to-go measurement are obtained from image frames. The second measurement, time-to-go, is closely related to target size and target expansion rate in the

image frames. Target size and its features are getting larger and obvious as the target getting close while LOS rate and bearing rate are decreasing. Therefore, the loss of observability at the last terminal guidance can be covered.

In section 2, time-to-go measurement has been derived from sequential image processing. The guidance filter dynamics are illustrated in section 3. Finally, numerical simulation results are shown in section 4.

2 Time-to-go Measurement

From EO/IR seeker, we can get sequential image frames including target feature. By some image processes, such as morphological filtering and CAM-Shift algorithm, we can track a target continuously. The target size and its expansion rate can be obtained from tracking results. The overall Sequential image processing are illustrated in Figure 1.

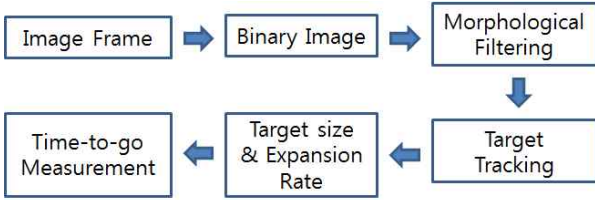


Figure 1 Image processing sequence for time-to-go measurement

2.1 Morphological Filtering

To extract target's feature from clutter and noise of image frames, preprocessing is required. In this study, we assume that a target could be distinguished from background due to the difference between target's intensity and the background intensity. At the first step, the morphological filter [4] is applied to extract target's feature. We use close morphological filtering. After the morphological process, the gray-scale image frames are filtered into binary images by given threshold. Therefore, pixels only containing the target are assigned 1 and background pixels are assigned 0. Figure 2 illustrates original input image frame and preprocessed binary image. The background feature has been removed by the filter.



Figure 2. Sample images:
(a) Gray-scale image,
(b) Preprocessed binary image

2.2 Tracking Algorithm

Continuously adaptive mean shift (CAM-Shift) algorithms are applied for tracking target in the preprocessed image sequences. CAM-Shift is a fundamental tracking algorithm for vision based target tracking. We assumed that target detection is already declared at actual target's location. CAM-shift algorithm only tracks the detected target using following steps [5].

CAM-Shift Algorithm

1. Determine a size of region of interest (ROI)
2. Determine the initial location of the ROI
3. Calculate the mean location of the ROI
4. Set the center of ROI at the mean location calculated in Step 3.
5. Repeat Step 3 and 4 until the mean location converges within a given threshold
6. Calculate a size of ROI from the zeroth moment

Repeat Step 2~6 continuously for each frame

The mean location of a ROI is determined by computing zeroth, and first order moment of a given image fame.

$$M_{00} = \sum_{x \in ROI} \sum_{y \in ROI} I_{pre}(x, y) \quad (1)$$

$$M_{10} = \sum_{x \in ROI} \sum_{y \in ROI} x I_{pre}(x, y) \quad (2)$$

$$M_{01} = \sum_{x \in ROI} \sum_{y \in ROI} y I_{pre}(x, y) \quad (3)$$

where $I_{pre}(x, y)$ is the preprocessed image frame. Here, the zeroth moment means size of the target in image frames. Then the mean ROI location is given by

$$x_c = \frac{M_{10}}{M_{00}}; \quad y_c = \frac{M_{01}}{M_{00}} \quad (4)$$

The size of ROI is determined larger than target's size which is given by

$$\text{width} = 2\sqrt{M_{00}}; \quad \text{height} = \sqrt{M_{00}}$$

Therefore, ROI can always include the entire target feature.

2.3 Calculation of Time-to-go Measurement

The target size in the each image frame is determined by zeroth order moment of the preprocessed image frame.

$$S_{\text{Target}} = \sum_{x \in \text{ROI}} \sum_{y \in \text{ROI}} I_{pre}(x, y) = M_{00} \quad (5)$$

Target expansion rates are defined as size difference between two consecutive frames, which is given by

$$\dot{S}_{\text{target}}(k\Delta T) = \frac{S_{\text{target}}(k\Delta T) - S_{\text{target}}((k-1)\Delta T)}{\Delta t} \quad (6)$$

where ΔT is sampling time interval for image sensor.

If the actual target size is invariant, target size in image frames, S_{target} , and range-to-go, r , are satisfying a following relationship;

$$S_{\text{Target}} = \frac{C}{r^2} \quad (7)$$

where C is a constant. By derivative of eq. (7), we can get following relationship between range-to-go, target size, and target expansion rate.

$$\begin{aligned} \dot{S}_{\text{Target}} &= -2 \frac{C}{r^3} \dot{r} \\ &= -2 \frac{S_{\text{Target}}}{r} \dot{r} \end{aligned} \quad (8)$$

$$\frac{\dot{S}_{\text{Target}}}{S_{\text{Target}}} = -2 \frac{\dot{r}}{r} \quad (9)$$

On the other hands, time-to-go can be expressed by range-to-go and its derivatives.

$$t_{go} = -\frac{r}{\dot{r}} \quad (10)$$

By substituting eq. (9) into eq. (10), we can construct a relationship between time-to-go, target size, and target expansion rate as follows

$$t_{go} = 2 \frac{S_{\text{Target}}}{\dot{S}_{\text{Target}}} \quad (11)$$

2.4 Low-pass Filtering

Target size is proportional to r^{-2} term. Target appears very small size in the image frame during most initial frames when relative range is large. On the other hands, target expansion rate is nearly zero for initial guidance, and it rapidly increases at the last final period. Therefore, just one pixel size error at initial period makes large estimation errors. To reduce the target size error effect, target size and target expansion rates are calculated by low-pass filtering. The iterative form of backward low-pass filter is given by

$$\tilde{S}_{\text{target}}(k\Delta T) = \frac{1}{1+a\Delta T} \tilde{S}_{\text{target}}((k-1)\Delta T) + \frac{a\Delta T}{1+a\Delta T} S_{\text{target}}(k\Delta T) \quad (12)$$

where a is a design parameter for cut-off frequency of low-pass filter.

After low-pass filtering, estimated target size are rounded off to the nearest integer. It means that sub-pixel sized target differences are not considered. However, by this rounding process, expansion rate error bounds are considered.

Figure 3 shows time-to-go measurement generated by integer target size and expansion

rate filtered by low-pass filter. Due to small target size small expansion rate for most initial period, time-to-go measurement has large initial errors. However, as the missile getting close to the target, measurement converges to true values.

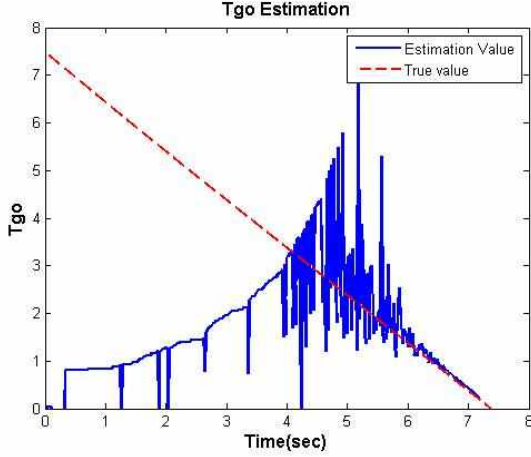


Figure 3. Time-to-go Measurement

3 Filter Equations

The Kalman filter dynamics have been constructed in Cartesian coordinate frame. In the Cartesian coordinate frame, equation of motion can be expressed as linear form. On the contrary, measurements dynamics will be expressed as nonlinear equation. Figure 4 illustrates the Cartesian coordinate frame.

The state variables are defined as relative distance and velocity between guided missile and the target

$$\mathbf{x}(t) \triangleq \begin{bmatrix} x & y & z & v_x & v_y & v_z \end{bmatrix}^T \quad (13)$$

Where

$$\begin{aligned} x &= x_T - x_M \\ y &= y_T - y_M \\ z &= z_T - z_M \\ v_x &= v_{T_x} - v_{M_x} \\ v_y &= v_{T_y} - v_{M_y} \\ v_z &= v_{T_z} - v_{M_z} \end{aligned}$$

The process equation is given by

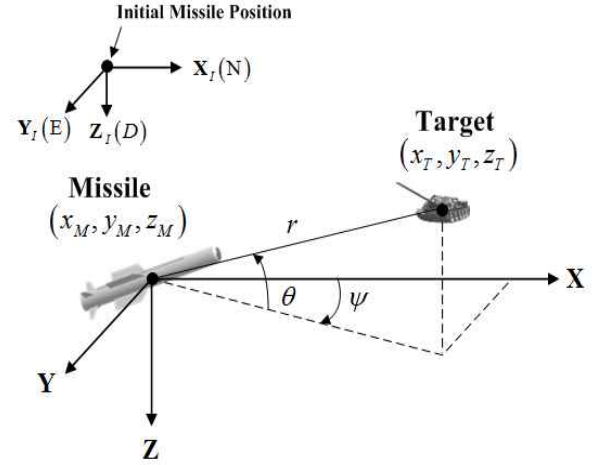


Figure 4. Coordinate Frame

$$\frac{d}{dt} \begin{bmatrix} x \\ y \\ z \\ v_x \\ v_y \\ v_z \end{bmatrix} = \begin{bmatrix} v_x \\ v_y \\ v_z \\ -a_{M_x} + w_x \\ -a_{M_y} + w_y \\ -a_{M_z} + w_z \end{bmatrix} \quad (14)$$

where $a_{M_x}, a_{M_y}, a_{M_z}$ are missile's acceleration of each direction and w is a process noise representing unconsidered target's motion.

Bearing angle and time-to-go measurements are used for a measurement set of extended Kalman filter. The measurements equation can be expressed as

$$\mathbf{z}(\mathbf{x}) = \begin{bmatrix} \theta_m \\ \psi_m \\ t_{go} \end{bmatrix} + \mathbf{v}$$

$$= \begin{bmatrix} \tan^{-1} \left(\frac{-z}{\sqrt{x^2 + y^2}} \right) \\ \tan^{-1} \left(\frac{y}{x} \right) \\ \frac{x^2 + y^2 + z^2}{v_x x + v_y y + v_z z} \end{bmatrix} + \mathbf{v} \quad (15)$$

4 Numerical Results

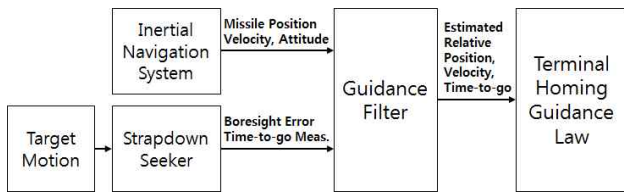


Figure 5. Configuration of Guidance Filter

To verify the performance of the filter, MATLAB Simulink based numerical simulations are constructed. The performances of filters using bearing-only measurement and using bearing and time-to-go measurement are compared by Monte-Carlo simulation.

The target location is (1960, 0, 20) and the initial position of the missile is (0, 0, 200). The update frequency of the seeker image is 50Hz. Guidance law is optimal guidance for impact angle control [6].

Figure 6 shows missile trajectories and its body angle changes.

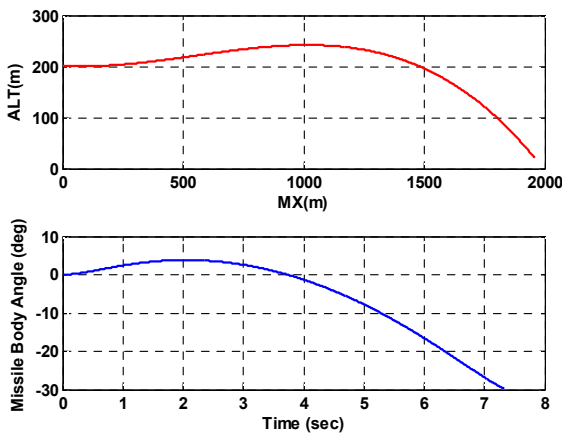


Figure 6. Missile trajectory and body angle

To compare performances of bearing-only measurement and bearing and time-to-go measurement, 200 times of Monte-Carlo simulation are conducted. The missile intercepts the target 7.4 sec after launch.

Results of the simulation are shown in Figure 7 and Figure 8. Figure 7 shows time-to-go estimation result and Figure 8 illustrates relative range estimation result.

For the detail comparison, average time-to-go and range-to-go estimation errors are shown in Figure 9 and Figure 10. Both time-to-go and range-to-go estimation errors are reduced by using time-to-go measurement from target size and its expansion rate. Although the time-to-go

measurements are not accurate until 4 seconds as shown in Figure 3, performance of the Extended Kalman filter is enhanced in terms of estimated range-to-go and time-to-go information.

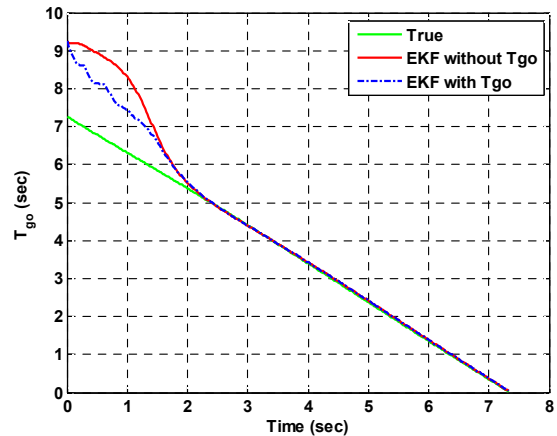


Figure 7. Time-to-go Estimation Results

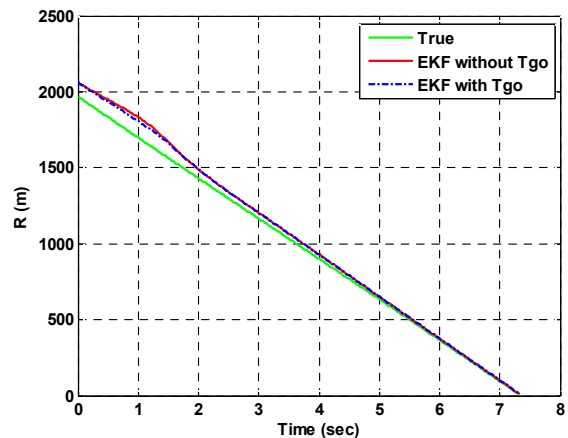


Figure 8. Relative Range Estimation Results

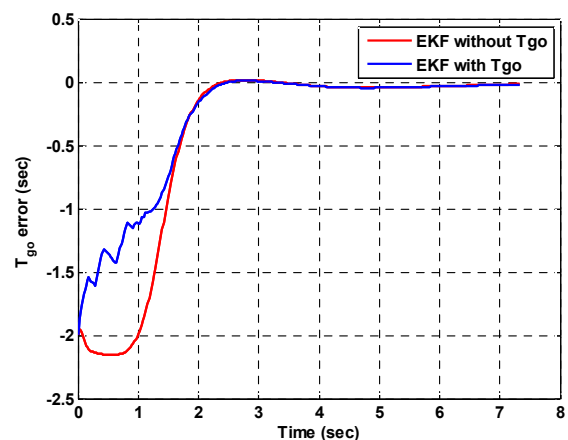


Figure 9. Time-to-go Estimation Errors

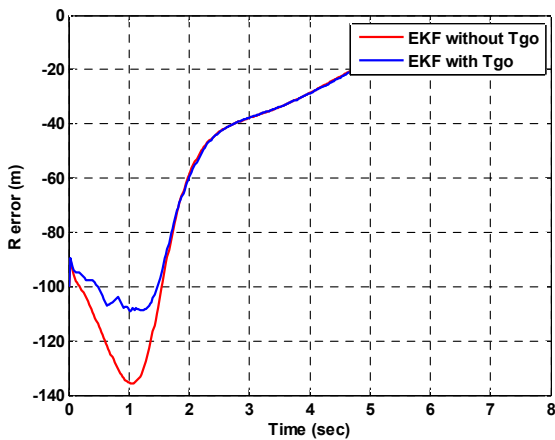


Figure 10. Relative Range Estimation Errors

5 Conclusion

In this paper, the extended Kalman filter dynamics are constructed using bearing measurement and time-to-go measurement in the Cartesian coordinate. Time-to-go measurements are obtained from the image frames of the passive seeker. The time-to-go measurements which are calculated from target size in image and its expansion rate are used. From numerical simulation, the estimation performance is enhanced by using additional time-to-go information.

References

- [1] Chang-Kyung Ryoo, Hangju Cho, Min-Jea Tahk. Time-to-go weighted optimal guidance with impact angle constraints. *Control Systems Technology, IEEE Transactions on*, vol.14, no.3, pp. 483- 492, May 2006.
- [2] Jin-Ik Lee, In-Soo Jeon, Min-Jea Tahk. Guidance law to control impact time and angle. *Aerospace and Electronic Systems, IEEE Transactions on*, vol.43, no.1, pp.301-310, January 2007.
- [3] Chang-Hun Lee, Min-Jea Tahk, Jin-Ik Lee. Generalized Formulation of Weighted Optimal Guidance Laws with Impact Angle Constraint, *Aerospace and Electronic Systems, IEEE Transactions on*, vol.49, no.2, pp.1317-1322, April 2013.
- [4] J. Serra. *Image Analysis and Mathematical Morphology*. London. U.K: Academic Press, 1982.
- [5] Dorin Comaniciu, Visvanathan Ramesh, P. Meer. Real-Time Tracking of Non-Rigid Objects using Mean Shift. *Computer Vision and Pattern*

Recognition, 2000. Proceedings. IEEE Conference on, Vol.2, pp. 142-149. 2000.

- [6] I. R. Manchester and A. V. Savkin, Circular-Navigation-Guidance Law for Precision Missile/Target Engagements, *Journal of Guidance, Control, and Dynamics*, Vol. 29, No. 2, pp. 314-320, March-April 2006.

Copyright Statement

The authors confirm that they, and/or their company or organization, hold copyright on all of the original material included in this paper. The authors also confirm that they have obtained permission, from the copyright holder of any third party material included in this paper, to publish it as part of their paper. The authors confirm that they give permission, or have obtained permission from the copyright holder of this paper, for the publication and distribution of this paper as part of the ICAS 2014 proceedings or as individual off-prints from the proceedings.